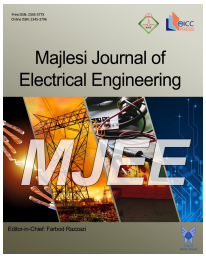

Majlesi J. Electr. Eng. 2026; 20(1) : 13-32

Majlesi Journal of Electrical Engineering (MJEE)

https://dx.doi.org/10.57647/mjee.2026.2001.02

Original Research

Optimal Sizing and Cost Reduction of Grid Tied Photovoltaic Battery Systems Using Artificial Protozoa Optimization

Devesh Jaiswal[1,*], Monika Mittal[1], Vikas Mittal[2]

[1]*Electrical Engineering Department, NIT KURUKSHETRA, Haryana, India*
[2]*Electronics and Communication Engineering Department, NIT KURUKSHETRA, Haryana, India*

[*]**Corresponding author:** devesh_61900069@nitkkr.ac.in

Article History

Received:
14 October 2024

Revised:
26 February 2025

Accepted:
12 April 2025

Published in Issue:
31 March 2026

Abstract:

This work focuses on optimal sizing of rooftop photovoltaic (PV) systems and battery energy storage systems (BESS) for grid-connected houses (GCHs) to minimize electricity costs under flat and time-of-use (TOU) rate structures. The research employs Artificial Protozoa Optimization (APO) algorithm to create a cost-effective optimization model, considering grid constraints, solar and load profiles, component costs, and degradation effects. Deep analyses explore the impact of electricity rate variations and grid limitations on system sizing and expenses. A rule-based energy organization system is used to optimize power flow amongst PV, BESS, load, and grid connections. The study compares Particle Swarm Optimization (PSO) and Artificial Protozoa Optimization (APO) algorithms across different tariff scenarios: flat-flat, TOU-flat, flat-TOU, and TOU-TOU. APO consistently outperforms PSO, achieving lower net present cost (NPC) and cost of energy (COE) while optimizing system power output and storage capacity. In various pricing scenarios, the APO algorithm consistently outperformed PSO, achieving significantly lower Net NPC and COE with optimized PV and BESS configurations. APO proved more effective in minimizing costs across TOU-TOU, flat-flat, and TOU-flat scenarios These findings highlight APO's superior performance in cost and efficiency optimization for grid-linked solar PV and BESS approaches.

Keywords: Battery energy storage system (BESS); Grid-connected houses (GCHs); Net present cost (NPC); Cost of energy (COE); Particle Swarm Optimization (PSO); Artificial Protozoa Optimization (APO)

Cite this article: Jaiswal D, Mittal M, Mittal V. Optimal Sizing and Cost Reduction of Grid Tied Photovoltaic Battery Systems Using Artificial Protozoa Optimization. Majlesi J. Electr. Eng. 2026;20(1): 13-32. https://dx.doi.org/10.57647/mjee.2026.2001.02

1. Introduction

The integration of rooftop solar photovoltaic systems with battery energy storage systems in grid-connected houses has gained significant attention as an effective solution for reducing electricity costs and enhancing energy sustainability. The economic viability of such Systems is highly influenced by electricity pricing structures, grid constraints, and component degradation over time. The worldwide on and off-grid PV installation is shown in figure 1. Around 99.6% of today's installed PV capacity is connected to the grid. The proportion of off-grid systems compared to the total cumulative systems has roughly halved over time from just under 1% in 2010 to 0.43% in 2023. India has achieved the 5th rank in the world in solar power deployment. As of 30-06-2023, solar projects of a capacity of 70.10 GW have been commissioned in the country. The capacity of 70.10 GW includes 57.22 GW from ground-mounted solar projects, 10.37 GW from rooftop solar projects, and 2.51 GW from off-grid solar projects from MNRE [1].

In [3], a new approach for optimizing the size of grid-connected PV systems for residential applications, specifically targeting a house in Tunisia, is presented. The objective of this work is to maximize system profitability and reliability over 20 years. The optimization implemented is PSO. This paper defined two multi-objective functions. The first aims to maximize the Net Present

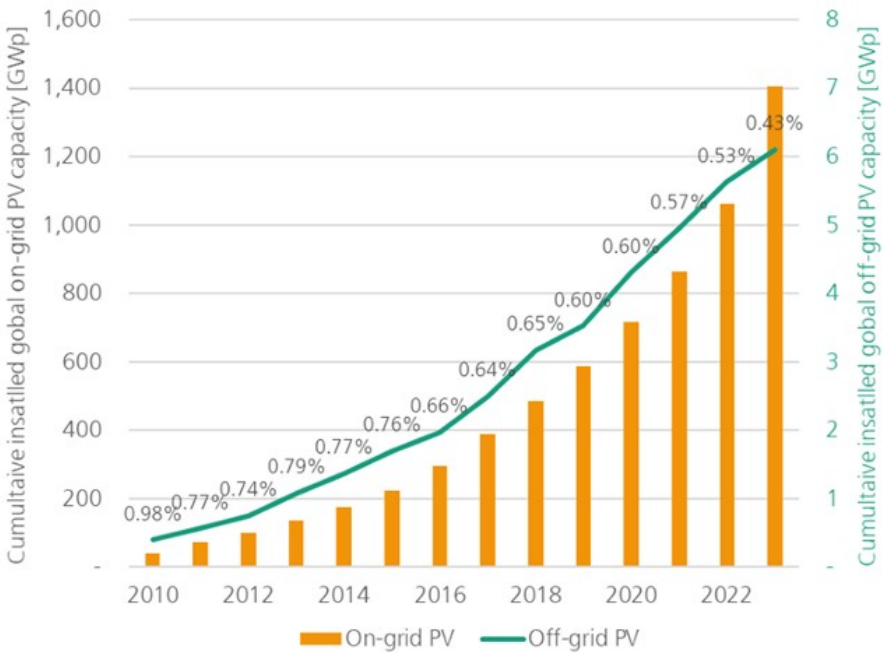

Figure 1. Global on-grid and off-grid PV installation [2].

Value (NPV), focusing on economic benefits, while the second aims to minimize the Loss of Power Supply Probability (LPSP). Simulation results showed that the PSO algorithm outperformed the Genetic Algorithm (GA) in terms of convergence speed and solution quality. The study concluded that PSO-based optimization is better suited for finding economically feasible solutions with minimal components, while minimizing LPSP leads to a more reliable but less profitable system. In [4], an energy management method in conjunction with the PSO algorithm was discussed to optimize energy cost. This work differed from prior studies by optimizing both PV and BESS sizes while using a grid-connected self-sustaining microgrid structure. The energy management algorithm is dynamic and can be reconfigured based on system constraints. In [5] the PSO method is implemented with a residential grid-linked PV system with proper power management in the battery during peak and off-peak hours. PSO method optimizes the battery capacity and reduces the operation cost. Real-time PV data from Strathmore University is demonstrated in this work.

In [6], the annual system cost (ASC) and loss of load supply probability (LLSP) are used to optimize PV energy cost and battery system. A hybrid optimization method was presented, combining simulated annealing and harmony search algorithms. Simulation results show that increasing PV and battery storage size enhances system reliability at a higher cost. The optimal operation of batteries in standalone and grid-connected microgrids was examined in [7]. Reducing energy losses in DC microgrids, decreasing CO_2 emissions from conventional generators, and lowering running costs are the target functions taken into consideration here. Three parallel optimization methods were used in the process: Parallel Ant Lion Optimizer (PALO), Parallel Vortex Search Algorithm (PVSA), and Parallel Particle Swarm Optimization (PPSO). The techniques are used to assess system performance and optimize hourly power flow. According to the results, efficiency is increased by employing parallel optimization techniques; PPSO performs better in reducing energy losses and operating expenses.

In [8], the optimization of PV and BESS sizing in grid-connected microgrids was discussed. An energy management strategy alongside the PSO algorithm to determine the optimal sizes of PV and BESS was discussed. The MG is designed to operate in both standalone and grid-connected modes, with limited grid energy demand to minimize costs. The study compares the PSO results with those obtained from the GA algorithm. The results suggest that a well-configured energy management system, combined with optimal PV and BESS sizing, can significantly reduce operational costs. In [9], the Grey Wolf Optimization (GWO) technique to address load dispatch issues and optimize microgrid performance by effectively sizing battery systems was discussed. The research compared GWO with other established optimization algorithms, such as GA, PSO, Bat Algorithm (BA), and Improved Bat Algorithm (IBA), across different operational scenarios. GWO demonstrates superior performance in terms of solution quality and computational efficiency. Simulation results show that GWO effectively reduces operational costs by 33.185% compared to the other methods. A comparison of ten metaheuristic optimization algorithms to solve the sizing problem for a standalone hybrid renewable energy system, incorporating PV/WT/Battery by [10]. The primary objective of the optimization is to minimize the total net present cost (TNPC) while maintaining system reliability, measured through the Deficiency of Power Supply Probability (DPSP). The study also considers additional criteria such as the levelized energy cost (LEC) and the relative excess

https://dx.doi.org/10.57647/mjee.2026.2001.02

power generated (REPG). Flower Pollination Algorithm (FPA) and Simulated Annealing (SA) emerged as the most reliable and accurate algorithms, with no deviation in the TNPC values across runs. SA demonstrated an optimal balance between robustness, accuracy, and speed, making it the best choice for solving the hybrid system's sizing problem. A new day-ahead scheduling model using the hybrid shuffled frog leaping and pattern search (HSFLA-PS) algorithm for a grid-connected microgrid is discussed in [11]. By considering real environmental data for different seasons and days, this approach improves the operational efficiency of the microgrid. The hybrid algorithm proves to be computationally efficient, providing accurate and optimized results. The study underscores the importance of managing uncertainties in DER outputs to enhance the reliability and performance of microgrids. Improved Harmony search algorithm is used in [12] to determine the size of BESS and with an objective function of minimizing total average operating cost. According to the availability of PV power, the BESS is optimized. A methodology for minimizing the operating costs of microgrids by optimizing the power allocation of distributed generators (DGs) and BESS was discussed in [13]. The use of Accelerated PSO, APSO, JAYA, and Linear Programming with Interior Point (LP-IP) algorithms is explored. Among these, the LP-IP approach demonstrates superior performance in reducing the overall operating cost while ensuring optimal sizing of BESS. The study highlights the significance of proper energy management techniques to maximize the benefits of microgrid operation, particularly in scenarios with intermittent renewable sources. In [14], the Tabu Search Algorithm (TSA) is employed to solve the optimal sizing problem for an off-grid clean microgrid system based on solar and battery energy storage. By minimizing the total life cycle cost and considering the reliability constraints, the study offers a comprehensive evaluation of the system's configuration. The TSA approach is effective in finding optimal solutions, making it suitable for rural areas with limited access to the main grid. The use of PSO for optimizing the size of microgrid components, including PV panels and BESS, to minimize the total annual cost (TAC) over a 20-year project lifetime was discussed in [15]. The PSO algorithm is compared with the Iterative Search Based (ISB) algorithm, with PSO showing faster simulation times and optimal BESS sizing to meet energy demands. The study by [16] explored the use of GWO and Whale Optimization Algorithm (WOA) to determine the optimal number of bifacial PV panels for grid-connected systems. The algorithms consider factors such as available space, energy production goals, and budget constraints. Both methods yield efficient and effective solutions, with WOA outperforming GWO in terms of optimization criteria. This research demonstrates the potential of advanced algorithms in enhancing the performance of solar energy systems and reducing overall costs. A Hybrid Grey Wolf Cuckoo Search Optimization (GWCSO) algorithm is presented for optimal sizing of system components, outperforming traditional GWO in minimizing costs and ensuring system robustness in [17]. The results show that GWCSO yields lower NPC and Levelized Cost of Energy (LCOE) compared to GWO, making it a more accurate and reliable optimization method for hybrid renewable systems. This study focuses on a hybrid grid-connected microgrid combining wind, PV, biomass, and energy storage systems. Diab et al. [18] addresses the design of a stand-alone microgrid for supplying safety loads during emergencies at a nuclear power plant in Egypt. The microgrid incorporates PV FC and battery storage. Three recent optimization algorithms Equilibrium Optimizer (EQ), Bat Optimization (BAT), and Black-Hole-Based Optimization (BHB) are applied to optimize the microgrid design. The Equilibrium Optimizer (EQ) algorithm delivers the best performance, offering the lowest objective function value. Although the cost of energy (COE) for the EQ-based design is slightly higher than that of the BAT algorithm, EQ's reliability index is superior, which justifies the higher COE. The integration of wind and PV, in grid-connected and stand-alone microgrids, was presented in [19]. Due to the intermittency of these resources, BESS is essential for ensuring grid stability. The paper investigates the required BESS sizes for both grid-connected and stand-alone configurations over 12 months, considering hourly wind power potential. Table 1 represents inference of various optimization methods used for optimal sizing and cost minimization.

In [20], a mixed linear integer problem, using intelligent control rules and optimization algorithms such as PSO, GA, and Flower Pollination Algorithm for the economic dispatch was presented. A case study based on data from Southwestern Australia demonstrates that intelligent control of batteries can significantly reduce the generation cost by 6.5% in islanded mode, 7.6% in grid-connected (no export) mode, and 11.5% in grid-connected (export) mode. The payback time for the investment in battery systems is shown to be approximately 2.7 to 2.8 years across all operating modes. In [22], a model of a hybrid microgrid that integrates PV, wind, and diesel generators along with battery storage was explored. The study aims to determine the optimal sizing of the microgrid components to minimize the COE while improving system reliability, measured by the loss of power supply probability. Several optimization algorithms are applied, including WOA, Water Cycle Algorithm (WCA), Moth-Flame Optimizer (MFO), and a hybrid Particle Swarm Optimization-Gravitational Search Algorithm (PSOGSA). In [21], the optimal design of a wind-battery hybrid microgrid system using various battery technologies, such as Nickel-Iron, Lithium-Ion, and Lead-Acid (LA) batteries, was examined. The focus is on reducing system costs and improving reliability in off-grid areas. The authors propose a mathematical model for assessing the operation cost and reliability, and they introduce an improved harmony search metaheuristic algorithm to optimize the system design. The method is compared with the original harmony search

https://dx.doi.org/10.57647/mjee.2026.2001.02

Table 1. Inference of various optimization methods used optimal sizing and cost minimization.

Ref No.	Sources Considered	Optimal Sizing	Methods Used	Cost Type	Target	Method Compared
[1]	PV	PV, BESS	PSO, GA	Net Present Value (NPV)	Maximize profitability, minimize LPSP	GA
[3]	PV and Battery	Battery capacity	PSO	Annual capacity cost	Minimize operation cost	-
[4]	PV and Battery	PV, Battery	Simulated Annealing, Harmony Search	Annual System Cost	Minimize system cost, LLSP	-
[5]	PV and Battery	Hourly power flow, Battery	PPSO, PVSA, PALO	Energy Fixed cost, Variable cost	Minimize energy losses, operating cost	PVSA, PALO
[6]	PV, Wind and Battery	PV, BESS	PSO, GA	Benefit-cost ratios and Net present value	Minimize costs	GA
[7]	PV, Wind, Fuel cell, Micro turbine and Battery	Battery	GWO	Best, Mean and Worst operation cost	Minimize operational costs	GA, PSO, BA, IBA
[8]	PV, WT, Battery	PV, WT, Battery	FPA, SA	TNPC	Minimize TNPC	-
[11]	Distributed generators and BESS	DGs, BESS	APSO, JAYA, LP-IP	Total operating cost for 24 hours	Minimize operating costs	JAYA, LP-IP
[12]	Off-grid PV and BESS	PV, BESS	Tabu Search Algorithm	Total life cycle cost	Minimize total cycle cost	-
[13]	PV, BESS	PV, BESS	PSO, Iterative-Based Search	Total Annual Cost	Minimize total annual cost	ISB
[14]	Grid-connected bifacial PV system and Inverter	PV, battery, Inverter	GWO, WOA	System, maintenance and replacement cost	Optimize energy production	GWO
[15]	Wind, PV, biomass, BESS	System components	GWCSO	NPC, LCOE	Minimize costs, ensure robustness	GWO
[16]	Standalone microgrid for a nuclear power plant	PV, Fuel Cells, BESS	Equilibrium Optimizer, Bat Optimization, Black Hole-Based Optimization	COE, Loss of power supply probability	Minimize costs during emergencies	BAT, BHB
[17]	PV with BESS for the isolated community	PV, BESS	Multi-Objective Particle Swarm Optimization	Operation cost of DG	Minimize cost, maximize reliability	-
[18]	PV, wind and Battery	PV, Wind, Battery	Enhanced Genetic Algorithm, SA	Levelized Energy Cost	Minimize LEC	SA
[20]	PV and BESS	PV, BESS	Artificial Bee Colony	NPC	Minimize NPC	-
[21]	Off-grid microgrid for rural electrification	PV, BESS	WOA, GA	TNPC	Minimize TNPC	GA

algorithm, showing a 13.5% reduction in total cost and 1.5% faster simulation time. A modified artificial bee colony optimization method to determine the optimal sizing, location, and scheduling of these systems to reduce costs and improve efficiency was presented in [23]. The study emphasizes load demand management, non-essential load shifting, and the use of Coulomb Counting for accurate battery estimation. It demonstrates the environmental benefits of integrating solar PV into rural energy systems, such as reduced CO_2 emissions and 24/7 power availability. An isolated microgrid in a remote area in Assiut, Egypt, which comprises a PV system, a diesel generator, and BESS was discussed in [24]. It presents a methodology to minimize the NPC using three meta-heuristic algorithms: GA, the crow-search algorithm (CSA), and GWO. The study compares these techniques to determine the optimal sizing of the diesel generator and BESS capacity, while considering operational costs, battery replacement, and system stability. PVSYST software is used to simulate the PV system, ensuring accurate results and factoring in shading losses.

An isolated microgrid in a remote area in Assiut, Egypt, which comprises a PV system, a diesel generator, and a BESS. was presented in [25]. It gives a methodology to minimize the NPC using three meta-heuristic algorithms: GA, CSA, and GWO. The review by [26] focuses on optimizing PV-battery systems in the residential sector to reduce electricity bills, grid dependence, and emissions. The paper identifies critical parameters influencing the planning process, including economic and technical factors, energy management systems, design constraints, and optimization algorithms. It also reviews state-of-the-art approaches and challenges in this field, emphasizing the need for new guidelines based on electricity rates and demand response programs.

In [27], an ensemble nonlinear model predictive con-

trol (EnNMPC) strategy is presented for short-term dispatch optimization, considering electricity trading costs, battery degradation, and operational constraints. This approach effectively minimizes operational costs despite uncertainties using real-world datasets. Similarly, in [28], a nonlinear model predictive control (NMPC) technique combined with dynamic programming has been used to optimize short-term power flow in PV-BESS systems, reducing electricity costs while mitigating battery degradation. These studies highlighted the importance of predictive control methods in ensuring cost-effective energy management. A study utilizing Walrus Optimization Algorithm (WaOA), Coati Optimization Algorithm (COA), and Osprey Optimization Algorithm (OOA) demonstrated significant cost reductions in a grid-connected hybrid system incorporating PV, wind, and fuel cell technologies. The results showed WaOA achieving a COE of 0.5175 $/kWh, outperforming traditional algorithms such as PSO and GWO [29]. While this study emphasizes multi-source energy integration, there is limited exploration of advanced metaheuristic techniques specifically for standalone PV-BESS systems. In [30], research on the technical-economic analysis of BESS sizing in energy markets has proposed a decision-support tool integrating Microsoft Excel and PowerApps to evaluate BESS feasibility for commercial consumers. By analyzing historical energy data over 8760 hours, this approach provides a practical framework for comparing BESS with diesel generators, demonstrating its viability in Brazil's free energy market. Several studies have explored performance assessment and optimization techniques for grid-connected solar PV systems to enhance energy generation and efficiency [31]. This research evaluates a 5 MW solar PV plant using PV system software and real-time SCADA data, highlighting the close correlation between simulated and actual performance metrics. Additionally, the study presented optimization using Tabu Search (TS) and PSO, concluding that PSO effectively maximizes energy output, financial returns, and reduces the payback period.

1.1 Problem statement

The integration of PV systems and battery energy storage (BES) has emerged as an important approach in modern energy management, particularly for grid-connected households aiming to reduce electricity costs and enhance sustainability. However, despite the increasing interest, there remain significant challenges in determining the optimal sizing and operation of these systems. Most studies have focused on specific geographic or economic conditions, such as in Tunisia or isolated microgrids, and often neglect the dynamic nature of energy prices, varying demand patterns, or grid conditions that affect system performance. Furthermore, the reliance on simplified assumptions, such as constant energy prices or limited consideration of battery degradation, may lead to suboptimal configurations that fail to address real-world complexities. There is also limited exploration of advanced metaheuristic algorithms for holistic optimization, which can offer superior performance in balancing cost minimization and energy efficiency in PV-BES integration. Additionally, challenges such as regulatory hurdles, system reliability, and the environmental impact of different configurations remain underexplored. Therefore, there is a need for a comprehensive approach that leverages modern optimization techniques to develop adaptable and cost-effective PV-BES systems for GCHs under diverse operating conditions.

To overcome the above problems, a new APO algorithm is proposed in [32]. The APO algorithm was chosen due to its ability to balance exploration and exploitation, preventing premature convergence and ensuring optimal solutions in nonlinear, multi-objective optimization problems like PV-BESS sizing. Compared to traditional methods such as PSO and GA, APO offers:

- Better adaptability to variable conditions such as dynamic energy pricing and demand variations.
- Improved efficiency in finding the global optimum, for its foraging, dormancy, and reproduction mechanisms inspired by protozoa.
- Faster convergence with lower computational cost, making it more suitable for real-time and complex optimization problems.

The novelty of this paper lies in the application of the APO algorithm for the optimal sizing and cost minimization of grid-connected solar PV and battery energy storage systems under various pricing structures. While many optimization techniques such as PSO, GA, and GWO have been explored in prior studies, this paper introduces APO, which improves exploration and exploitation balance, avoids local optima, and dynamically adapts to environmental conditions. The comparative analysis with PSO demonstrates APO's superior performance in terms of NPC, COE and energy exchange between PV, BESS, and the grid.

1.2 Contribution

The main contribution of the paper is given as follows,

- Developed an optimal sizing methodology for grid-connected PV-BESS systems under four different pricing models (Flat-Flat, TOU-Flat, Flat-TOU, TOU-TOU), addressing cost-effectiveness in variable electricity pricing scenarios, which has not been extensively explored in prior works, especially for Indian residential energy consumers.
- Introduced APO as a novel metaheuristic optimization technique for PV-BESS system sizing, offering superior global search capability compared to existing methods. Demonstrated APO's effectiveness over traditional algorithms (PSO, GA, GWO) by achieving better convergence, avoiding local optima, and dynamically adapting to cost variations and environmental conditions.
- Conducted a detailed performance comparison of APO and PSO across multiple tariff structures,

proving APO's superiority in reducing NPC and COE. Results showed that APO reduced NPC and COE, highlighting its better optimization efficiency and energy management performance.

- Conducted a case study using real-world Indian pricing and weather data, incorporating power flow analysis, battery state of charge (SOC) trends, and sensitivity analysis. Addressed practical challenges, including battery degradation, grid constraints, and energy import/export optimization, providing comprehensive insights for residential PV-BESS deployment.

1.3 Structure of the paper

The paper is organized into the following sections: The review of various algorithms used in optimal sizing is presented in section 1. Section 2 describes the energy management in the proposed system and the objective function. Section 3 and 4 provides a detailed analysis optimization model and proposed APO algorithm and PSO for optimal sizing. A case study and simulation analysis and its results is presented in section 5 and 6 respectively. A summary of the work done is presented in section 7.

2. Energy management

A grid-linked PV scheme integrated with rooftop solar panels is represented in figure 2. The PV modules convert sunlight into electrical energy, which is then fed into an inverter. The inverter transfers the DC into AC energy, making it suitable for household use and capable of being fed into the grid. The PV scheme is linked to the primary electrical grid, which can accept surplus power produced by the PV system or deliver electricity to the household load. The load consists of the domestic electrical devices or appliances that consume power. The power flows within the system are represented by various symbols: P_o indicates the output power from the inverter, which can be focused on either the load or the grid; P_L is the power provided to the load. P_i is the power imported after the grid to change the load demand when the PV production is inadequate. P_e is the excess power exported to the grid when the PV generation surpasses the load demand and P_d signifies the power that is dumped or curtailed. Dumped power indicates any excess power that is not used by the load or exported to the grid, which can occur due to system constraints or inefficiencies. This diagram illustrates the balance and flow of electrical energy between the rooftop PV scheme, the load, and the grid, highlighting how surplus power can be managed and utilized within the system.

The power flow involving the PV, load, and grid is managed by the Home Energy Management System (HEMS). In this setup, excess power is sold to the grid while taking the grid constraint into account if the power generated by the PV (P_o) is more than the domestic load (P_L). As a result, the price of selling power to the grid (P_e) may be expressed in equation (1)

$$P_e(t) = P_o(t) - P_L(t) \tag{1}$$

The excess electricity from rooftop photovoltaics is discarded if it surpasses the grid constraint ($P_{e,\max}$). It should be noted that the inverter's control system dumps the power that is considered dumped; this power is not a bodily burden. Equation (2) gives formula that can be used to get the dumped power (P_d):

$$P_d(t) = P_o(t) - P_L(t) - P_{e,\max} \tag{2}$$

However, if the electricity supplied by the rooftop photovoltaic system is insufficient to cover the load, the excess power needs to be bought from the grid. Equation (3) represents the purchased power (P_i) from the grid:

$$P_i(t) = P_L(t) - P_o(t) \tag{3}$$

Figure 3 represents an enhanced grid-linked PV scheme that integrates rooftop solar panels and a battery storage

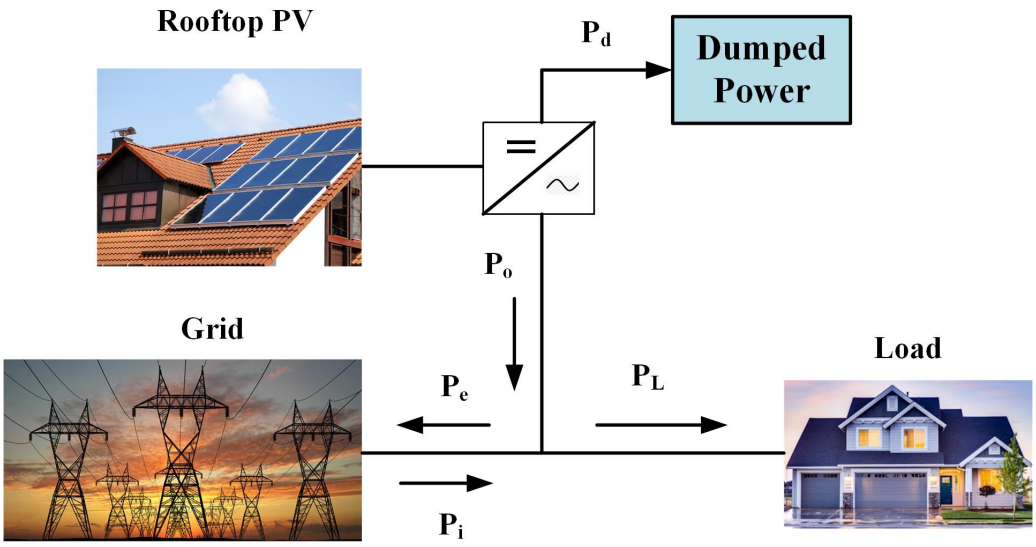

Figure 2. Grid-linked PV, Grid and Load.

https://dx.doi.org/10.57647/mjee.2026.2001.02

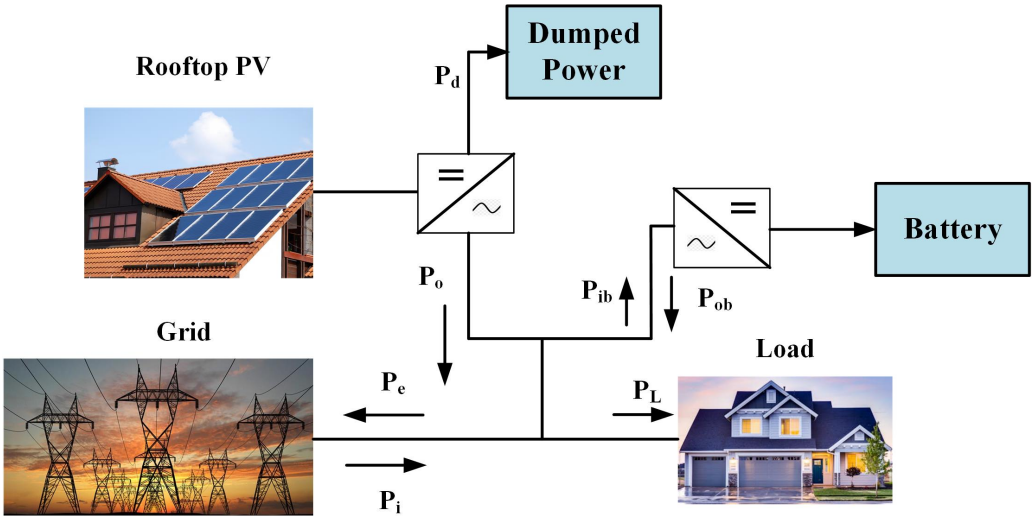

Figure 3. Grid-linked PV, Grid, load with battery.

system. The rooftop PV panels convert sunlight into electrical power, which is then fed into an inverter to be converted into AC power, making it suitable for household use and grid integration. This scheme is linked to the main electrical grid, allowing for bidirectional power flow. The components and power flows include the rooftop PV panels generating DC power, the inverter converting DC to AC power, and the battery storage system managed by an additional inverter. The main electrical grid can supply power to the household load or receive excess power produced by the PV scheme. The household load consists of electrical devices or appliances that consume power. The power flows are represented as follows: P_o is the yield power from the primary inverter, directed to the load, the grid, or the battery system; P_L is the power supplied to the load, P_i is the power imported from the grid when PV generation and battery supply are insufficient, P_e is the surplus power exported to the grid when PV generation exceeds load demand and battery storage is full, P_d is the power dumped or curtailed, representing excess power not used by the load, stored in the battery, or exported to the grid, P_{ib} is the power directed to the battery for charging; and P_{ob} is the power output from the battery to supply the load or support the grid.

The HEMS regulates the flow of electricity between the PV, BESS, load, and grid in this system. When the rooftop PV system's produced power surpasses the load, the excess power first charges the BESS while taking the battery's available input power limit into account. The battery's (P_{ib}) charging power can be expressed in equation (4):

$$P_{ib}(t) = P_o(t) - P_L(t) \tag{4}$$

When PV power surpasses the battery's load and input power limits, surplus power is offered to the grid while taking grid constraints into account. The power management is represented from equations (5) to (11). The exported electricity to the grid is represented as

$$P_e(t) = P_o(t) - P_L(t) - P_{ib}(t) \tag{5}$$

The following is how more power can be released

$$P_d(t) = P_o(t) - P_L(t) - P_{ib}(t) - P_{e,\max} \tag{6}$$

However, if the power provided by the PV scheme is insufficient to connect the load, the BESS's discharge power can make up the difference, considering the battery's maximum output power. The battery's (P_{ob}) discharging power may be written as follows:

$$P_{ob}(t) = P_L(t) - P_o(t) \tag{7}$$

If the battery's maximum output power is insufficient to meet the whole load, the shortfall is imported from the grid in the manner described below:

$$P_i(t) = P_L(t) - P_o(t) - P_{ob}(t) \tag{8}$$

For every period (Δt), the SOC of the battery is determined by

$$SOC(t+\Delta t) = SOC(t) + \frac{(P_{ib}(t)\eta_{ib} - \frac{P_{ob}(t)}{\eta_{ob}})\Delta t}{E_b} \tag{9}$$

where E_b is the battery capacity and η_{ib} is the import efficiency of the battery. The BESS power (P_{ib}) and power output (P_{ob}) available limitations are determined by

$$P_{ib}(t) = \frac{E_b}{\Delta t}(SOC_{\max} - SOC(t)) \tag{10}$$

$$P_{ob}(t) = \frac{E_b}{\Delta t}(SOC(t) - SOC_{\min}) \tag{11}$$

3. Optimization model

The model's objective function, the system's design restrictions, and the optimization process are all included in the ideal sizing.

https://dx.doi.org/10.57647/mjee.2026.2001.02

3.1 Objective function

The main objective is to reduce the overall NPC. The NPC of factors (NPC_s) and the NPC of electricity replacement with the grid (NPC_g) may be used to calculate the total NPC (NPC_t) in the following equation (12)

$$NPC_t = NPC_s + NPC_g \tag{12}$$

The NPC of components may be determined using the capital cost (PC_c), replacement current cost (PC_r), maintenance current cost (PC_m), and the redemption value of PV and BESS.

Thus, the following formula (equation (13)) may be used to get the NPC_s:

$$NPC_s = N_b \left(PC_{c(b)}\right) + PC_{m(b)} + PC_{r(b)} - PC_{s(b)}\big) + N_{pv} \left(PC_{c(pv)}\right) + PC_{m(pv)} + PC_{r(pv)} - PC_{s(pv)}\big) \tag{13}$$

where the BESS and PV systems are denoted by the subscripts b and pv, respectively, and N_b, N_{pv} are the number of components in the battery and PV system. The initial project expenditure is known as the investment cost for PV and BESS. Equation (14) may be used to determine the components' replacement current cost:

$$PC_m = C_m \frac{1}{(1+ir)^M} \tag{14}$$

The equation (15) can be used to calculate the elements' present maintenance costs:

$$PC_r = C_r \frac{(1+ir)^M - 1}{ir(1+ir)^M} \tag{15}$$

The components' salvation value can be stated using equation (16):

$$PC_s = N * PC_c \times \frac{R}{M'} \tag{16}$$

where R is the component's remaining lifespan after the project's lifetime and M is its lifetime. PV expertise lifespan is typically specified by the manufacturer. However, the capacity degradation during system operation determines the BESS lifespan, which is attained when the deterioration reaches 20%. Based on a battery's state of charge (SOC), the depth of discharge (DOD) is used to compute the capacity degradation of BESS.

$$DOD(t) = 1 - SOC(t) \tag{17}$$

Determining the number of cycles and the corresponding DOD is necessary to compute battery deterioration. This study used the Rainflow cycle counting technique to obtain all battery cycle data from the yearly DOD. The appropriate experimental model was developed using the calendar lifetime and accelerated experimental cycle testing under various stress components and stress levels of BESS acquired. For the system's yearly operation, the total deterioration of the battery (TBD) is represented as follows:

$$TBD = \sum_{c} BD(c) \tag{18}$$

where, $BD(c)$ is the battery degradation for each cycle.

Typically, the rate of inflation (er) that drives up the cost of power is higher than the rate of interest (ir). As a result, the interest rate on electricity (ie) may be written like this:

$$ie = \frac{ir - er}{1 + er} \tag{19}$$

The following formula is used to determine the NPC of electricity as a purpose of the new interest rate on electricity and the yearly power cost:

$$NPC_g = C_g \frac{(1+ie)^n - 1}{ie(1+ie)^n} \tag{20}$$

The yearly cost of electricity, or C_g, is determined by factoring in the electricity that is bought, sold, and the rates that go along with it.

$$C_g = \sum_{t=1}^{K} I(t)P_i(t) \times \Delta t - \sum_{t=1}^{K} E(t)P_e(t) \times \Delta t \tag{21}$$

Design limitations

The constructed optimization model was subject to several design limitations, which are outlined below equations (22)-(26).

$$0 \le P_o(t) \le P_{o,\max} \tag{22}$$

$$0 \le P_{ib}(t) \le P_{ob}(t) \text{ and } 0 \le P_{ib}(t) \le P_{ob}(t) \tag{23}$$

$$SOC_{\min} \le SOC(t) \le SOC_{\max} \tag{24}$$

$$P_b(t) + P_{ot}(t) + P_i(t) - P_e(t) \ge P_L(t) \tag{25}$$

$$0 \le P_e(t) \le P_{e,\max} \tag{26}$$

3.2 Cost of electricity

The relationship of net yearly expenditure to net annual residential power usage is known as the COE. The following formula is used to determine the COE, which was utilized to compare the calculated procedures in this analysis:

$$COE = \frac{NPC_s \times CRF_s + NPC_g \times CRF_g}{E_L} \tag{27}$$

The following formula is used to determine the GCH's yearly electricity demand (E_L):

$$E_L = \sum_{t=1}^{K} P_L(t) \times \Delta t \tag{28}$$

Component and power exchange costs have distinct formulas for the capital recovery factor (CRF).

$$CRF_s = \frac{dr(1+dr)^n}{(1+dr)^n - 1'} \tag{29}$$

$$CRF_g = \frac{de(1+de)^n}{(1+de)^n - 1} \tag{30}$$

4. Artificial protozoa optimizer

This section provides an overview of the APO procedure, starting with an explanation of its source. We then provide geometric methods that simulate protozoa.

https://dx.doi.org/10.57647/mjee.2026.2001.02

Inspiration

Microorganisms such as bacteria, algae, and protozoa achieve tasks like those of organs in larger organisms through specialized structures called organelles. They exhibit fundamental life traits like metabolism, reproduction, genetic continuity, diversity, and stimulus-response, and are often used in studies due to their simpler organization. It exhibits both plant-like and animal-like characteristics, obtaining nutrients autotrophically from minerals or heterotrophically from organic substances. In unfavorable conditions, Euglena forms a cyst and becomes dormant. It reproduces asexually through binary fission.

Euglena has applications in environmental biomediation and biomedicine. It serves as a pointer of ecological strength, assesses water quality, resists heavy metals, and restores contaminated water. It contains euglenophycin, a toxin with anticancer properties, and is an ingredient of single-cell proteins used in drugs and commercial products like dietary supplements, food additives, and cosmetics. Further details on euglena's behaviors are explored through algebraic models in the following section. Figure 4 represents the Euglena cells, showing the main organelles.

Foraging

Euglena acquires essential nutrients via autotrophic and heterotrophic processes. It implements photosynthesis with chloroplasts to produce energy, like plants. Phototaxis, or movement in response to light, is guided by an eyespot that filters light to the photoreceptor at the flagellum's base. Under low light, euglena moves toward the light, while high irradiance causes it to move away to protect its pigments and chloroplasts. The threshold for switching between positive and negative phototaxis is between 10 and 100 W/m^2, allowing euglena to find optimal light conditions for photosynthesis. In darkness, euglena absorbs organic matter through phagocytosis, demonstrating animal-like behavior. Unlike plant cells, euglena has a flexible pellicle instead of a rigid cellulose wall, enabling free deformation and nutrient absorption through osmotrophic. This dual nutrient acquisition ability highlights its adaptability and survival in various environments.

Dormancy

Under diverse conditions, such as pollution in the environment, fluctuations in temperature, or scarcity of food organisms can adapt and survive in different ways. Certain animals move to lessen the stress they face from their surroundings, while others modify their innate behavior to stay out of trouble. Euglena can spray mucus subcutaneously in reaction to adverse circumstances, generating a protective mucilaginous capsule known as a cyst. The euglena goes into dormancy currently till the surrounding ecological circumstances improve. The initial cell loses its flagella and changes into ovoid, elliptical, and spherical forms. Euglena changes from a motile, single-cellular organism to a mucus colony that is not motile. The euglena's metabolism slows down in this state of suspended animation, which helps it conserve energy and become less dependent on the outside world. Euglena has the adaptive ability to respond to environmental stressors by going into dormancy.

Reproduction

Binary fission is a basic asexual reproductive mechanism seen in euglena. The euglena divides into two identical individuals throughout this process. Euglena reproduction is best suited for temperatures between 20 and 35 °C. Binary fission includes the reproduction of the flagellum, esophagus, and stigma and starts with the euglena nucleus going through mitosis. The cell divides again, this time along its longitudinal axis. The V-shaped bifurcation begins as a split at the front and moves progressively toward the posterior until the two sections are fully divided.

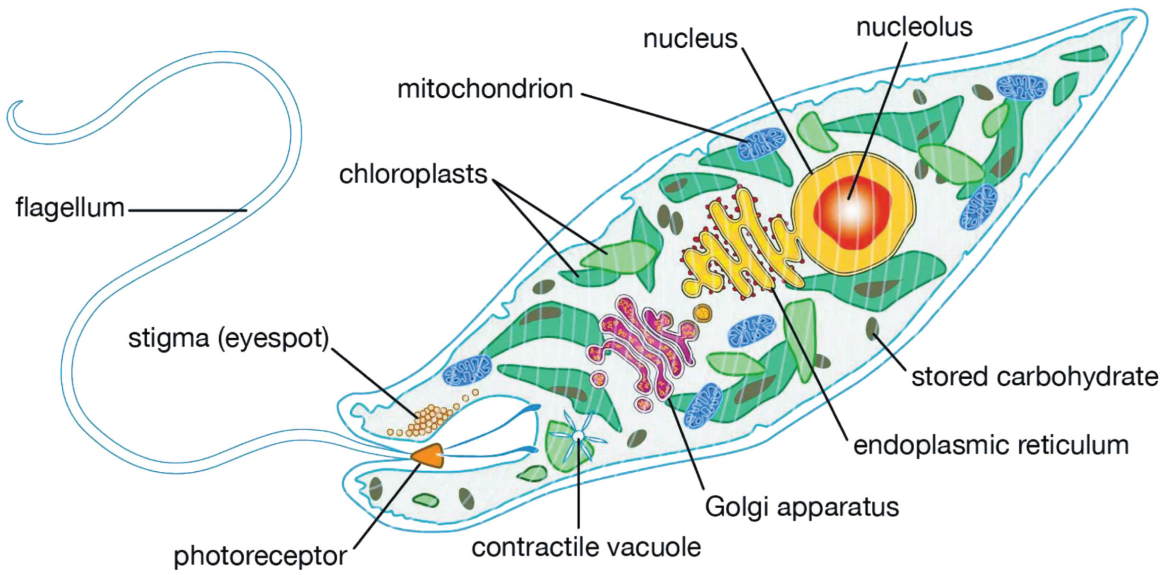

Figure 4. Euglena cell showing the main organelles [27].

https://dx.doi.org/10.57647/mjee.2026.2001.02

Mathematical models

The minimization problem's algorithm is introduced in this subsection. The solution set is represented by the protozoa in this suggested method, and each protozoan has a location made up of *dim* variables.

Foraging

Considering both the protozoa's internal and exterior elements while analyzing foraging behavior. The protozoa's foraging traits are considered internal variables, whereas environmental impacts such as species collisions and competing behaviours are considered external ones.

Autotrophic mode

Protozoan can obtain nourishment by using their chloroplasts to generate carbohydrates. The protozoan will migrate away from its current place and near a site with lower light intensity if it is exposed to bright light. When it is in an area with minimal light intensity, the opposite is true. The protozoan will migrate to the site of the j^{th} protozoan if the light intensity surrounding it is appropriate for photosynthesis. We offer the following mathematical model for the autotrophic mode:

$$X_i^{new} = X_i + f(X_j - X_i + \frac{1}{np}.\sum_{k=1}^{np}\omega_a \times (X_{k^-} - X_{k^+})) \odot M_f \tag{31}$$

$$X_i = [x_i^1, x_i^2, \ldots, x_i^{dim}], X_i = sort(X_i) \tag{32}$$

$$f = rand.\left(1 + \cos(\frac{iter}{iter_{max}} \times \pi)\right) \tag{33}$$

$$np_{\max} = \lfloor \frac{ps-1}{2} \rfloor \tag{34}$$

$$\omega_a = e^{-|\frac{f(x_{k^-})}{f(x_{k^+})+eps}|} \tag{35}$$

$$M_f[di] = \begin{cases} 1, & if\ di\ is\ in\ randperm(dim\lceil dim \times \frac{i}{ps} \rceil \\ 0, & otherwise. \end{cases} \tag{36}$$

where X_i^{new} and X_i stand for the protozoan's original position and updated position, respectively. Are the protozoan chosen at random, an arbitrarily chosen protozoan in the k^{th} paired neighbour with a rank index less than i is indicated by the symbol X_{k^-}. To be more precise, if $X_i = X_1$, then $X_{k^-} = X_1$. An arbitrarily chosen protozoan in the k^{th} paired neighbour is indicated by X_{k^+}, and its rank table is higher than i. $X_i = X_{ps}$ means that $X_{k^+} = X_{ps}$, where ps represents the population size. Foraging factors are represented by f, and random numbers in the [0,1] interval from the even distribution are denoted by rand. The current and maximum iterations are indicated by $iter$ and $iter_{max}$, respectively.

The maximum value of np is $np_{\max}$, and np represents the number of neighbour pairs outside the external components. In the autotrophic mode, ω_{ps} (2.2204e-16) It is a remarkably tiny quantity, and ω_a is a weight factor.

Heterotrophic mode

A protozoan may get nourishment in the dark by taking up organic materials from its environment. Presuming that X_{near} is a close-by area rich in food, the protozoan advances in its direction. We offer the following mathematical model for the heterotrophic mode:

$$X_i^{new} = X_i + f(X_{near} - X_i + \frac{1}{np} \times \sum_{k=1}^{np}\omega_h \times (X_{i-k} - X_{i+k})) \odot M_f \tag{37}$$

$$X_{near} = \left(1 \pm Rand \times \left(1 - (\frac{iter}{iter_{max}})\right)\right) \odot X_i \tag{38}$$

$$\omega_h = e^{-|\frac{f(x_{i-k})}{f(x_{i+k})+eps}|} \tag{39}$$

$$Rand = [rand_1, rand_2, \ldots, rand_{dim}] \tag{40}$$

where $''\pm''$ indicates that X_{near} may be in another direction from the i^{th} protozoan and X_{near} is a neighbouring place. The $(i-k)^{\text{th}}$ protozoan chosen from the k^{th} matching neighbor is indicated by the symbol $X_{i-k'}$, and its rank index is $i-k$. If $X_i = X_1$, then $X_{i-k}$is likewise set to X_1. The $(i+k)^{\text{th}}$ protozoan chosen from the k^{th} paired neighbour is indicated by the notation $X_{i+k'}$, and its rank index is $i+k$. The weight component in the heterotrophic mode is denoted by ω_h. The elements of the random vector Rand are in the [0,1] interval.

Dormancy

A protozoan may go dormant as a means of surviving adverse environmental circumstances while under stress. To keep the population steady, a freshly created protozoan replaces the dormant protozoan. The following is the mathematical model of dormancy,

$$X_i^{new} = X_{\min} + Rand \odot (X_{\max} - X_{\min}) \tag{41}$$

$$X_{\min} = [lb_1, lb_2, \ldots, lb_{dim}],\ X_{max} = [ub_1, ub_2, \ldots, ub_{dim}] \tag{42}$$

where the lower- and upper-bound vectors are denoted, respectively, by $X_{\min}$ and $X_{\max}$. The variables lb and ub denote the variable's lower and upper limits, respectively.

Reproduction

Binary fission is the asexual reproduction process that protozoa go through when they reach an adequate age and state of health. In theory, the protozoan splits into two identical daughters because of its reproduction. By creating a replica protozoan and taking a perturbation into account, we were able to imitate this behavior. The following is the reproduction mathematical model:

$$X_i^{new} = X_i \pm rand(X_{\min} + Rand \odot (X_{\max} - X_{\min})) \odot M_r \tag{43}$$

$$M_r[di] = \begin{cases} 1, & if\ di\ is\ in\ randperm(dim\lceil dim \times rand \\ 0, & otherwise. \end{cases} \tag{44}$$

where $''\pm''$ denotes the possibility of both forward and backward perturbations. In the reproduction process, M_r is a representing vector with a size of $(1 \times dim)$, Each element has a value of 0 or 1.

https://dx.doi.org/10.57647/mjee.2026.2001.02

Algorithm

The APO's particulars are displayed below. The following parameters must be considered to integrate all mathematical models:

$$pf = pf_{\max} \times rand \tag{45}$$

$$p_{ah} = \frac{1}{2} \times \left(1 + \cos\left(\frac{iter}{iter_{\max}} \times \pi\right)\right) \tag{46}$$

$$p_{dr} = \frac{1}{2} \times \left(1 + \cos\left(\left(1 - \frac{1}{ps}\right) \times \pi\right)\right) \tag{47}$$

where pf is the maximum value of pf and $pf_{\max}$ is the percentage fraction of dormancy and reproduction in the protozoa inhabitants. The probability of autotrophic and heterotrophic activities is shown by p_{ah}, whereas the probabilities of dormancy and reproduction are indicated by p_{dr}. It should be noted that the suggested APO only has two unique parameters: the maximum proportion fraction p_{ah} and the number of neighbour pairs N_p. Figure 5 depicts the APO algorithm's structure.

4.1 PSO optimization in optimal sizing and cost minimization

The PSO algorithm is a popular method for solving optimization problems related to optimal sizing and cost minimization of grid-connected solar PV and BESS. PSO is particularly useful due to its simplicity and efficiency in exploring a wide solution space for finding the optimal configuration of PV and battery systems.

Working mechanism of PSO for optimal sizing and cost minimization:

1. Initialization: PSO begins by initializing a population of particles, each representing a potential solution for the system configuration. A particle's position is described by a vector that includes decision variables like the solar PV capacity and battery storage size. These particles are initialized randomly within the defined limits for PV and BESS.

2. Fitness Evaluation: The objective is to minimize the NPC, which includes both the upfront and operational costs over the lifetime of the system. Each particle's fitness is evaluated based on the NPC or other financial indices like the COE.

3. Particle Movement and Update: In PSO, each particle adjusts its position based on its own experience (personal best, p_{best}) and the experience of the entire swarm (global best, g_{best}). The velocity and position of each particle are updated using the following equations:

$$v_i(t_i + 1) = \omega v_i(t_i) + c_1 r_1 (p_{best} - x_i(t_i)) + c_2 r_2 (g_{best} - x_i(t_i)) \tag{48}$$

$$x_i(t_i + 1) = x_i(t_i) + v_i(t_i + 1) \tag{49}$$

- $v_i(t_i)$ is the velocity of particle (i) at iteration (t_i),
- $x_i(t_i)$is the position of particle (i) at iteration (t_i),
- ω is the inertia weight,
- c_1 and c_2 are the cognitive and social coefficients,
- r_1 and r_2 are random numbers between 0 and 1.

Convergence: Over iterations, the particles' positions converge towards the best solution, representing the optimal sizing of PV and BESS that minimizes costs. The balance between exploration (searching new areas of the solution space) and exploitation (refining current best solutions) helps ensure that the algorithm doesn't get stuck in local minima.

Cost minimization:

In the context of cost minimization, PSO ensures that the NPC of the PV and battery system is minimized while meeting the energy demand. The sizing of the PV system affects the generation capacity, and the battery storage size affects how energy is stored and dispatched, impacting overall costs and self-consumption ratios.

PSO's efficiency in searching large solution spaces makes it ideal for scenarios where system components, costs, and grid conditions are variable. Through PSO, an optimal solution can be identified that balances the capital cost, operating costs, and energy savings, making it a highly effective tool for optimal sizing of grid-connected solar PV and battery storage systems. In summary, PSO uses a population-based approach with velocity and position updates to identify the optimal configuration of PV and BESS systems that minimizes the Net Present Cost, ensuring the most cost-effective design for grid-connected solar energy applications.

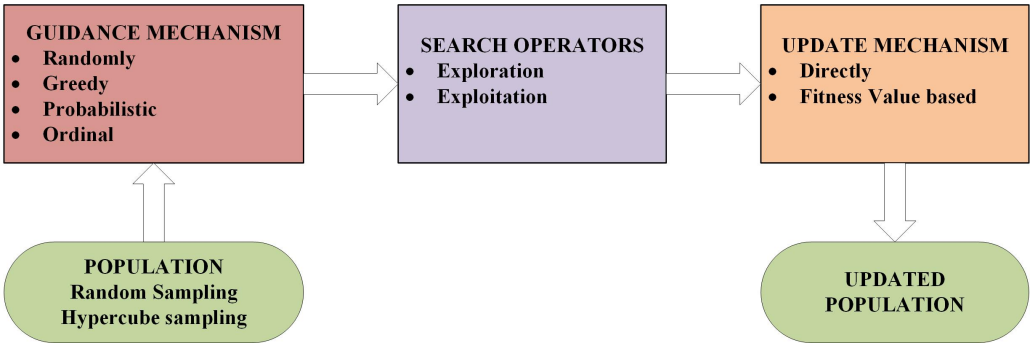

Figure 5. Framework of the proposed algorithm.

5. Case study

An analysis of the ideal size model was conducted for an Indian case study. This was accomplished by taking the weather and electrical usage data from a typical GCH in India. parameters with the ideal case study size.

Table 2 provides key parameters necessary for determining the optimal sizing of a system that integrates grid export limits and energy management. The grid export limit is set to 5 kW, which restricts how much energy can be fed back into the grid. The project uses an escalation rate of 2%, representing the annual increase in costs, and an interest or discount rate of 8% for economic calculations. Electricity purchase charges are Rs 7 per kWh, and selling charges (the price at which excess electricity is sold back to the grid) are Rs 5.6 per kWh. The project is evaluated over a lifetime of 20 years, providing a long-term perspective for cost and benefit analysis.

Table 3 presents the electricity exchange rates for both purchasing and selling under different pricing schemes for the proposed Energy Management System (EMS). The flat rate for electricity purchase is Rs 7 per kWh and Rs 5.6 per kWh for selling. Additionally, time-of-use (TOU) rates vary depending on the time of day: during peak hours, the purchase rate is Rs 8.45 per kWh and the selling rate is Rs 5.92 per kWh. During shoulder periods, these rates drop to Rs 5.82 per kWh for purchasing and Rs 3.29 per kWh for selling, while during off-peak times, the purchase rate is Rs 3.70 per kWh and the selling rate is Rs 1.64 per kWh. This dynamic pricing allows the EMS to optimize energy usage based on time-sensitive electricity costs.

Figure 6 and figure 7 represents the annual variations of Electricity Consumption and PV irradiance respectively.

Table 4 presents the characteristics and cost details for an ideal sizing model of a rooftop photovoltaic scheme combined with a BESS. The PV scheme, with a unit size of 1 kW, has a capital cost of Rs 83,400 per kW, a replacement cost of Rs 16,700 per kW, and an annual maintenance cost of Rs 2,750 per kW, with a lifespan of 20 years. The BESS, sized at 1 kWh/0.5 kW, has a capital cost ranging from Rs 3,900 to Rs 55,600 per kWh, a replacement cost of Rs 22,240 per kWh, no maintenance cost, and a lifespan of 20 years.

6. Results and discussion

This section evaluates the power flow analysis, sensitivity evaluation, and ideal outcomes for both system configurations. Table 5 lists the four alternatives for which the results are displayed, based on the rates at which power is purchased and sold.

Optimal sesults of system configurations

The optimization outcomes for each power rate choice for both system configurations are presented: Rooftop PV and BESS capacity at maximum efficiency, (a) total NPC of system configurations (c) The systems' COE; (d) The energy imported from the grid each year (AIEG); (e) The energy sent to the grid each year (AEEG); It should be mentioned that all of the economic values in this study are displayed in Indian Rupees (INR).

6.1 Option 1: Flat-Flat

Table 6 compares the results of two optimization algorithms PSO and APO, in determining the optimal sizing of the PV and BESS under a flat rate scheme for both buying and selling electricity. PSO suggests a system with 6 kW of PV and 19 kWh of BESS, leading to a NPC_t of Rs 86,387.6783, a COE of Rs 18.58 per kWh, and an annual imported energy from the grid (AIEG) of 0.024483 MWh. APO, on the other hand, proposes an 8 kW PV system and an 8 kWh BESS, resulting in a much lower NPC_t of Rs 38,266.7875, a COE of Rs 6.48 per kWh, and significantly higher values for both AIEG and annual exported energy to the grid (AEEG) at 1.7727 MWh and 10.8747 MWh, respectively. This highlights APO's ability to achieve more cost-effective results and better energy exchange.

Table 2. Parameters considered for optimal sizing.

Specification	Value
Grid export limit (kW)	5
Escalation rate (%)	2
Interest/ Discount Rate (%)	8
Electricity Purchase charges (Rs/kWh)	7
Electricity Selling charges (Rs/kWh)	5.6
Project lifetime (years)	20

Table 3. Economic data of the proposed EMS.

Electricity Exchange	Purchasing (Rs/kWh)	Selling (Rs/kWh)
Flat rates	7	5.6
TOU rates during Peak	8.45	5.92
TOU rates during Shoulder	5.82	3.29
TOU rates during Off-peak	3.70	1.64

https://dx.doi.org/10.57647/mjee.2026.2001.02

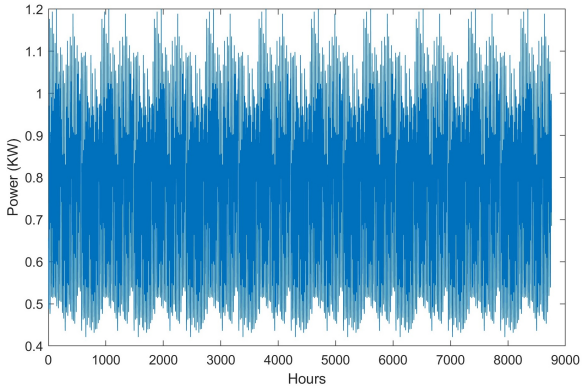

Figure 6. Annual variations of electricity consumption.

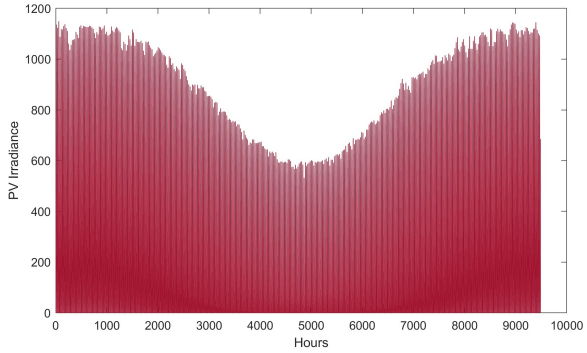

Figure 7. Annual variations of PV irradiance.

For the PSO optimization, the PV system produces 6 kW of power, and the BESS has a capacity of 19 kWh. The total net present cost is 86,387.6783 rupees, with a cost of energy at 7,085.32 Rs/kWh.

The annual increment in energy generation is 0.024483 MWh, and the annual energy export to the grid is 5.6418 MWh.

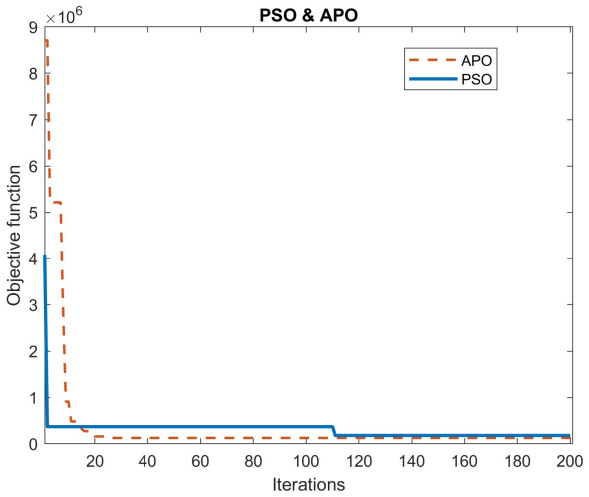

Figure 8. Objective function vs Iteration for APO and PSO during option 1.

In contrast, the APO optimization results show an 8 kW PV system with an 8 kWh BESS. The total net present cost is significantly lower at 38,266.7875 rupees, with a cost of energy at 2,742.42 Rs/kWh. The annual increment in energy generation is considerably higher at 1.7727 MWh, and the annual energy export to the grid is 10.8747 MWh.

Figure 8 likely illustrates the convergence behavior of the objective function over iterations for both the APO and PSO algorithms. It highlights how each optimization technique progresses towards the optimal solution, with APO showing a more rapid or stable convergence compared to PSO. Figure 9 demonstrates the distribution and flow of power within the system when optimized using PSO under flat-flat conditions. It would typically show how the generated power is allocated between consumption, storage, and export to the grid. Figure 10 focuses

Table 4. Rooftop PV and BESS characteristics for the ideal sizing model.

Component	Unit Size	Capital cost	Replacement cost	Maintenance cost	Lifetime
PV	1 kW	Rs 83400/kW	Rs 16700/kW (for Inverter in 10th year)	Rs 2750/kW/year	20 years
BESS	1 kWh/0.5 kW	Rs3900-55600/kWh	Rs 22240/kWh	NIL	20 years

Table 5. Options for retail pricing and feed-in tariff depending on the kind of power.

Options	Retail Price	Feed-in- Tariff
1	Flat	Flat
2	TOU	Flat
3	Flat	TOU
4	TOU	TOU

Table 6. Optimal results compared with PSO and APO optimization (Flat-Flat).

Optimization	PV (kW)	BESS (kWh)	NPC_t	COE(Rs/kWh)	AIEG(MWh)	AEEG(MWh)
PSO	6	19	86387.6783	18.58	0.024483	5.6418
APO	8	8	38266.7875	6.48	1.7727	10.8747

https://dx.doi.org/10.57647/mjee.2026.2001.02

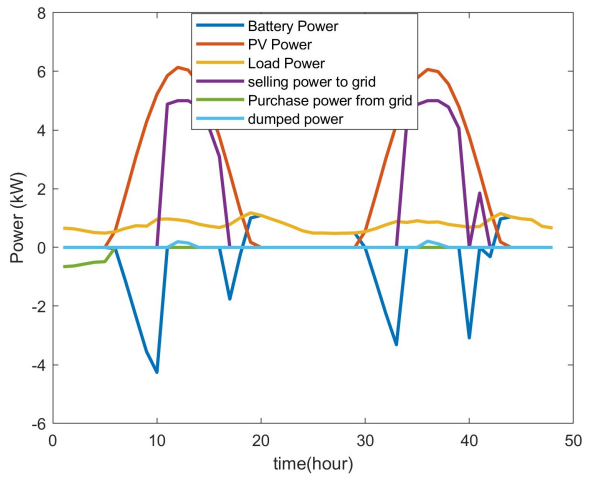

Figure 9. Power flow analysis during flat-flat using PSO.

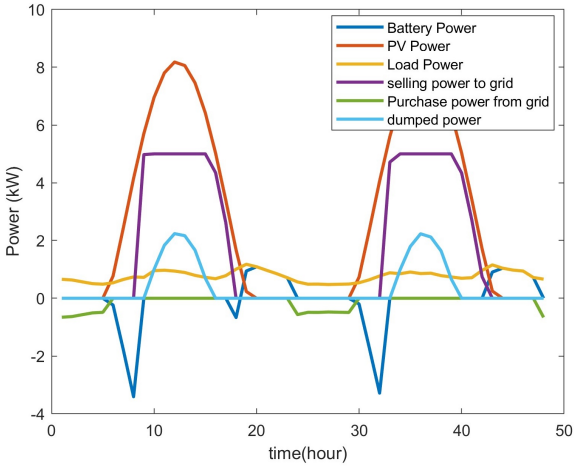

Figure 10. Power flow analysis during flat-flat using APO.

on the power distribution and flow within the system optimized using APO. It would likely show improvements in efficacy and excellent utilization of sources compared to the PSO method. Figure 11 illustrates the SOC of the BESS over time for both APO and PSO optimizations. It highlights the differences in how each method manages battery storage, with APO possibly showing a more efficient or stable SOC profile compared to PSO. These analyses and figures collectively demonstrate the superior performance of APO over PSO in terms of lower costs, higher energy generation, and better management of energy resources under flat-flat conditions.

6.2 Option 2: TOU-Flat

Table 7 compares the optimization results of PSO and APO for a system with time-of-use rates for purchasing electricity and flat rates for selling. PSO recommends a system with 9 kW of PV and 9 kWh of BESS, leading to a NPC_t of Rs 44,809.2447 and a COE of Rs 8.54 per kWh. The system imports 1.5541 MWh from the grid annually and exports 11.6839 MWh. APO, on the other hand, suggests a 5 kW PV system with the same 9 kWh BESS, reducing the NPC_t to Rs 36,389.309 and the COE to Rs 7.93 per kWh. Despite having a slightly higher imported energy (1.5628 MWh), the exported energy drops to 5.414 MWh, indicating that APO optimizes the system for better cost savings while reducing energy exports.

Figure 12 illustrates how the objective function, representing the optimization goal (such as cost minimization or efficiency maximization), evolves over iterations for both the APO and PSO algorithms. It demonstrates the convergence patterns of each method, showing how they progress towards the optimal solution. APO might exhibit a faster or more stable convergence compared to PSO, indicating its efficiency in reaching optimal results. Figure 13 shows the distribution and flow of power within the system optimized using PSO under TOU-Flat conditions. It details how the generated power from the PV system is utilized, gathered in the BESS, or exported to the grid, providing insights into the efficiency and effectiveness of the PSO optimization in managing energy

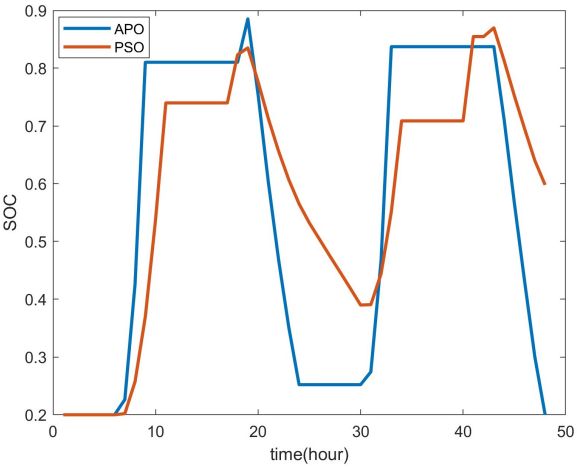

Figure 11. SOC of APO and PSO during flat-flat.

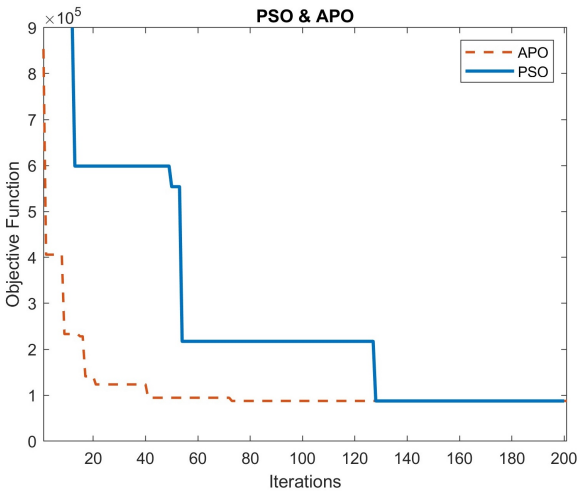

Figure 12. Objective function vs iteration for APO and PSO during option 2.

resources. Figure 14 represents the power distribution and flow within the system optimized using APO. It highlights improvements in efficiency, better utilization of the PV system, and more effective management of the BESS compared to the PSO method. Figure 15

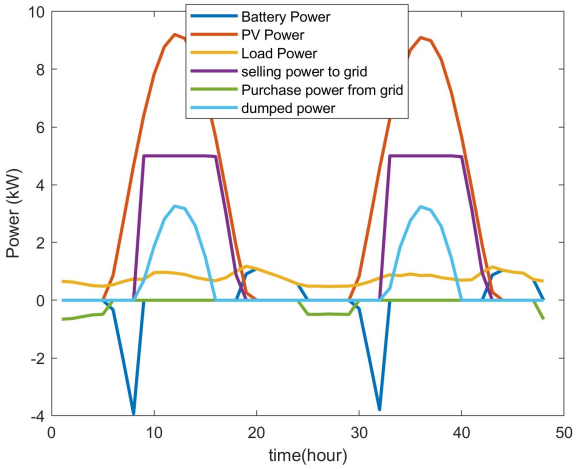

Figure 13. Power flow analysis during TOU-flat using PSO.

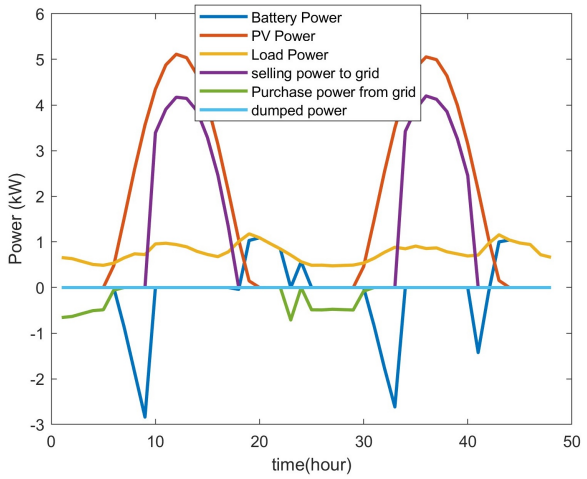

Figure 14. Power flow analysis during TOU-flat using APO.

illustrates the SOC of the BESS over time for both APO and PSO optimizations under TOU-Flat conditions. It shows how each optimization technique manages the battery's charge and discharge cycles, with APO potentially displaying a more stable or efficient SOC profile, leading to better overall system performance.

Overall, these analyses and visual representations highlight the superior performance of APO over PSO in optimizing energy resources under TOU-Flat conditions, with lower costs, higher energy generation, and improved management of the PV system and BESS.

6.3 Option 3: Flat-TOU

Table 8 shows the comparison between PSO and APO optimization under a flat rate for purchasing electricity and a time-of-use rate for selling. PSO once again suggests a system with 9 kW PV and 9 kWh BESS, resulting in an NPC_t of Rs 44,809.2447 and a relatively high COE of Rs 11.46 per kWh. The system imports 1.5541 MWh and exports 11.6839 MWh annually. APO, however, opts for a smaller 5 kW PV system while maintaining the same BESS size, lowering the NPC_t to Rs 36,389.309 and the COE to Rs 9.93 per kWh. The imported energy remains almost the same at 1.5628 MWh, while the exported energy drops significantly to 5.414 MWh, indicating a more balanced approach that favors a lower cost of energy and reduced exports.

Figure 16 illustrates the progression of the objective

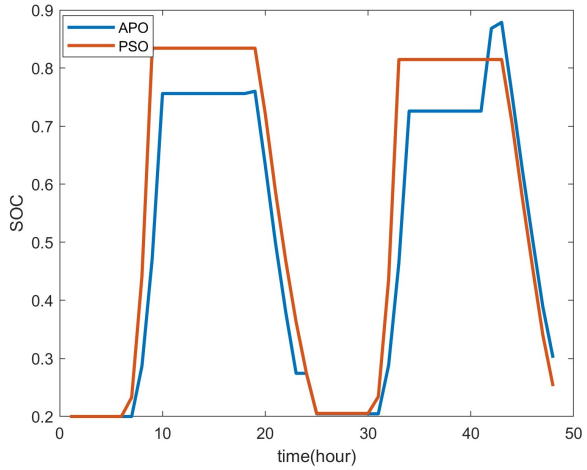

Figure 15. SOC of APO and PSO during TOU-flat.

function, representing the optimization goal (such as minimizing costs or maximizing efficiency), over iterations for both the APO and PSO algorithms. It demonstrates how each method converges towards the optimal solution. The convergence patterns may reveal that APO achieves faster or more stable convergence compared to PSO, indicating its superior efficiency in reaching optimal results. Figure 17 shows the distribution and flow of power within the system optimized using PSO under Flat-TOU conditions. It details how the power

Table 7. Optimal results compared with PSO and APO optimization (TOU-Flat).

Optimization	PV (kW)	BESS (kWh)	NPC_t	COE(Rs/kWh)	AIEG(MWh)	AEEG(MWh)
PSO	9	9	44809.2447	8.54	1.5541	11.6839
APO	5	9	36389.309	7.93	1.5628	5.414

Table 8. Optimal results compared with PSO and APO optimization (Flat-TOU).

Optimization	PV (kW)	BESS (kWh)	NPC_t	COE(Rs/kWh)	AIEG(MWh)	AEEG(MWh)
PSO	9	9	44809.2447	11.46	1.5541	11.6839
APO	5	9	36389.309	9.93	1.5628	5.414

https://dx.doi.org/10.57647/mjee.2026.2001.02

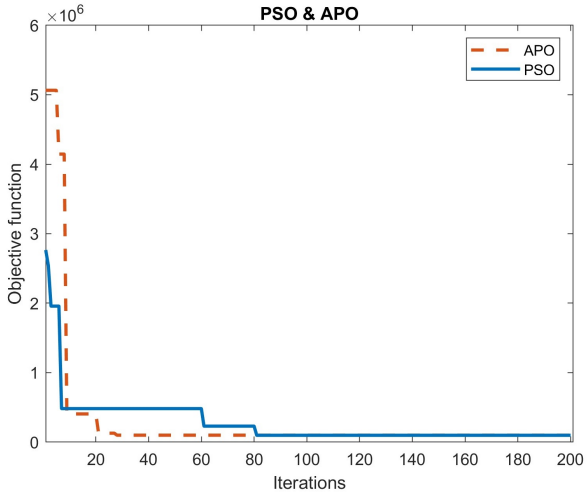

Figure 16. Objective function vs iteration for APO and PSO during option 3.

generated from the PV system is utilized, saved in the BESS, or exported to the grid. This provides insights into the effectiveness and effectiveness of the PSO optimization in managing energy resources. Figure 18 focuses on the power distribution and flow within the system optimized using APO. It highlights improvements in efficiency, better utilization of the PV system, and more effective management of the BESS compared to the PSO method. Figure 19 illustrates the SOC of the BESS over time for both APO and PSO optimizations under Flat-TOU conditions. It shows how each optimization technique manages the battery's charge and discharge cycles, with APO potentially displaying a more stable or efficient SOC profile, leading to better overall system performance. Overall, these analyses and visual representations underscore the superior performance of APO over PSO in optimizing energy resources under Flat-TOU conditions. APO demonstrates lower costs, higher energy generation efficiency, and improved management of the PV system and BESS.

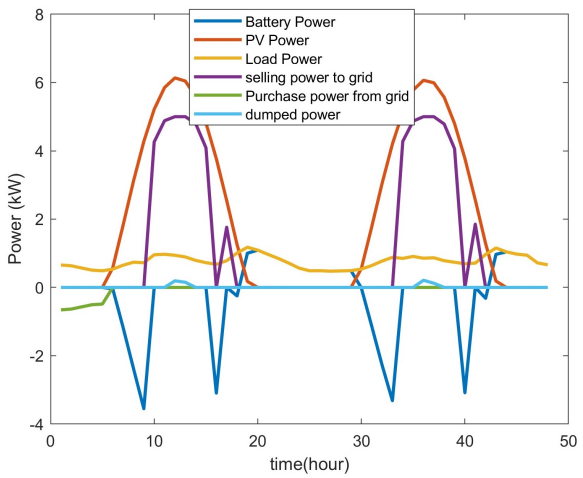

Figure 17. Power flow analysis during flat-TOU using PSO.

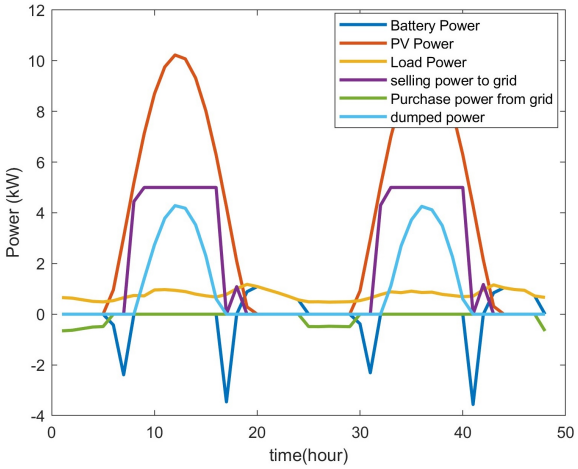

Figure 18. Power flow analysis during flat-TOU using APO.

6.4 Option 4: TOU-TOU

Table 9 presents optimization results for a system under TOU rates for both purchasing and selling electricity. PSO proposes a system with 9 kW PV and 9 kWh BESS, resulting in an NPC_t of Rs 44,809.2447 and a COE of Rs 8.54 per kWh. The system imports 1.5541 MWh from the grid and exports 11.6839 MWh annually. APO, on the other hand, significantly reduces the PV size to 2 kW while keeping the BESS at 9 kWh. This results in a much lower NPC_t of Rs 24,842.2996 and a drastically reduced COE of Rs 2.86 per kWh. Although APO's system imports more energy (2.5682 MWh) and exports much less (0.088446 MWh), it achieves a much lower overall cost, demonstrating its efficiency in cost reduction for systems with TOU pricing schemes.

To validate the effectiveness of the proposed APO, The APO algorithm is run 10 times for 200 iterations with population size of 100 as represented in figure 20 The global optimal is between 50 to 125 iterations. Table 10 shows the computation time and fitness for 10 APO runs.

The Mean (Average) Fitness Value is 87570.44 and the Standard Deviation is 0.26. The Mean (Average) computational Time is 129.25 seconds and Standard

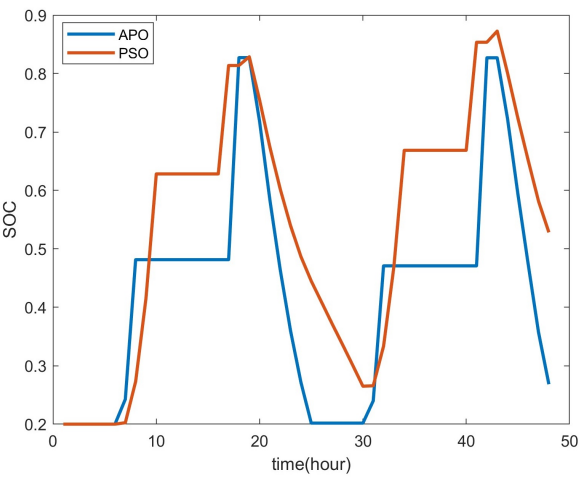

Figure 19. SOC of APO and PSO during flat-TOU.

Table 9. Optimal results compared with PSO and APO optimization (TOU-TOU).

Optimization	PV (kW)	BESS (kWh)	NPC_t	COE(Rs/kWh)	AIEG(MWh)	AEEG(MWh)
PSO	9	9	44809.2447	8.54	1.5541	11.6839
APO	2	9	24842.2996	2.86	2.5682	0.088446

Deviation is 3.23 seconds. The best fitness is chosen based on the best fitness value with minimal iterations.

Figure 21 illustrates the progression of the objective function, which represents the optimization goal (such as minimizing costs or maximizing efficiency), over iterations for both the APO and PSO algorithms. It demonstrates how each method converges towards the optimal solution. The convergence patterns may reveal that APO achieves faster or more stable convergence compared to PSO, indicating its superior efficiency in reaching optimal results. Figure 22 shows the distribution and flow of power within the system optimized using PSO under TOU-TOU conditions. It details how the power generated from the PV system is utilized, saved in the BESS, or exported to the grid. This provides

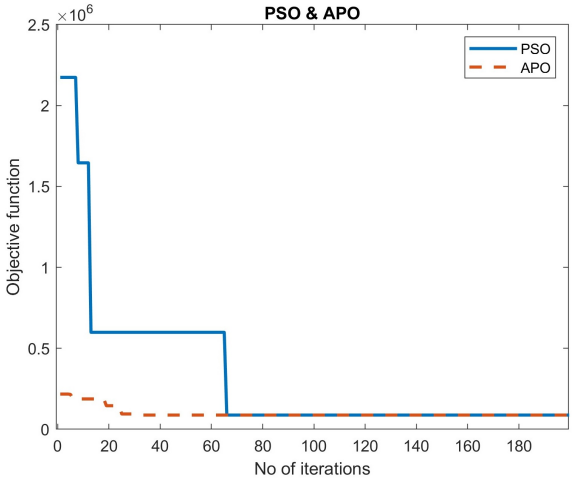

Figure 20. Objective function vs iteration for APO and PSO during option 4.

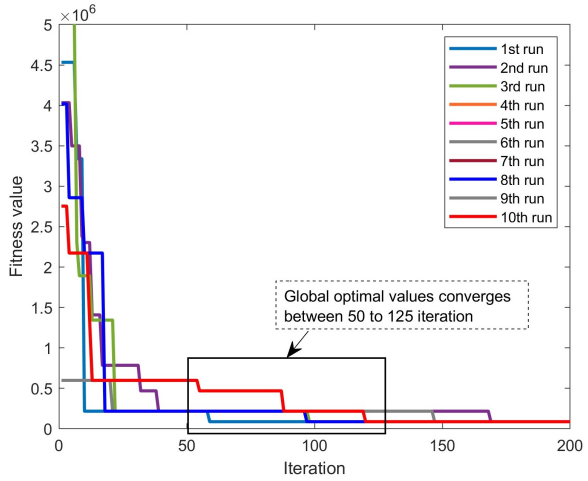

Figure 21. Convergence of APO for 10 independent runs.

Table 10. Computation time and Fitness value for 10 APO runs.

Number of Runs	Fitness value	Time (s)
1	87570.3	125
2	87570.5	134
3	87570.5	131
4	87570	128
5	87570.3	129
6	87570.9	134
7	87570.3	126
8	87570.3	127
9	87571	132
10	87570.3	128

perceptions of the competence and effectiveness of the PSO optimization in managing energy resources under variable TOU tariffs. Figure 23 focuses on the power distribution and flow within the system optimized using APO. It highlights improvements in efficiency, better utilization of the PV system, and more effective management of the BESS compared to the PSO method. The analysis shows how APO optimizes energy usage and storage to minimize costs and maximize energy generation under TOU-TOU conditions. Figure 24 illustrates the SOC of the BESS over time for both APO and PSO optimizations under TOU-TOU conditions. It shows how each optimization technique manages the battery's charge and discharge cycles. The SOC profile for APO may demonstrate more stable or efficient charge and discharge patterns, leading to better overall system performance and reduced costs.

Overall, these analyses and visual representations underscore the superior performance of APO over PSO in optimizing energy resources under TOU-TOU conditions.

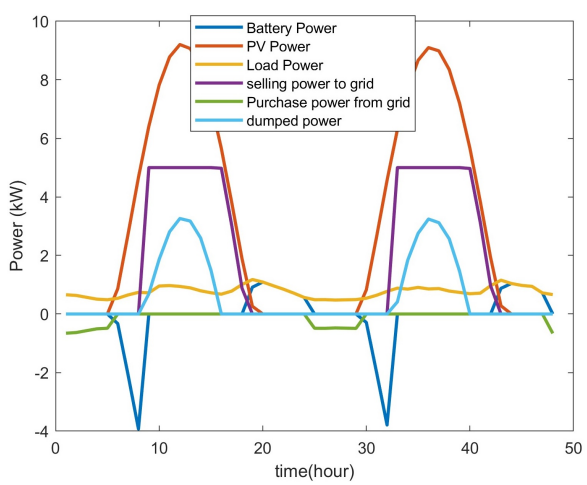

Figure 22. Power flow analysis during TOU-TOU using PSO.

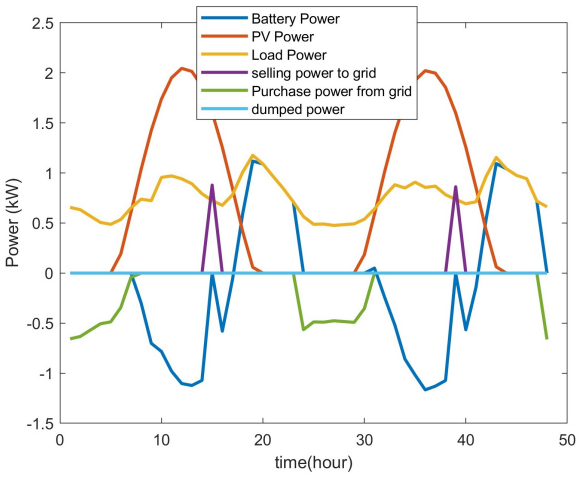

Figure 23. Power flow analysis during TOU-TOU using APO.

APO demonstrates lower costs, higher energy generation efficiency, and improved management of the PV scheme and BESS, making it a more effective optimization method for energy systems under variable TOU tariffs.

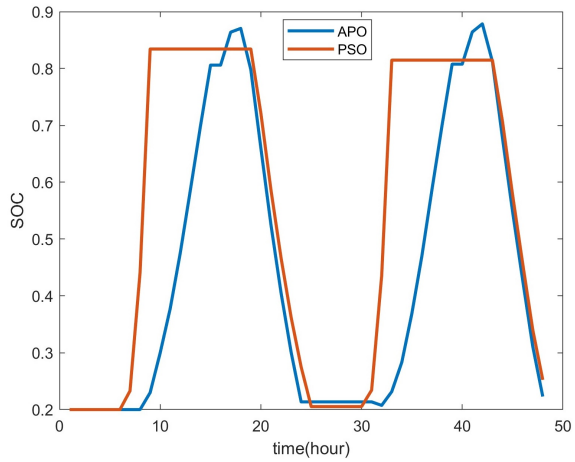

Figure 24. SOC of APO and PSO during TOU-TOU.

6.5 Sensitivity analysis

Sensitivity analysis for TOU-TOU conditions is carried out to validate the system, here, the computational parameters are varied (i.e Export power and TOU multiplier). Figure 25 illustrates the sensitivity analysis of export power limitations on a PV-BESS system, where the x-axis represents the export power limitation in kW, and the y-axes represent power, BESS capacity, and the COE in Rs/kWh. As the export power limitation increases, the optimal PV capacity also increases, starting from around 2 kW at 0 kW export limitation and reaching approximately 8 kW at 10 kW. This aligns with the observation that grid constraints reduce the optimal PV size. The BESS capacity remains nearly constant at 6 kWh across all export power limits, indicating minimal impact on battery sizing. Meanwhile, the COE decreases as the export limit increases, starting at around 7.5 Rs/kWh when export is restricted and dropping to 1 Rs/kWh when full export is allowed. This confirms that limiting grid export leads to higher COE due to lower PV utilization, whereas greater export flexibility makes the system more cost-effective. The analysis highlights the economic and technical effects of grid constraints on PV-BESS system performance.

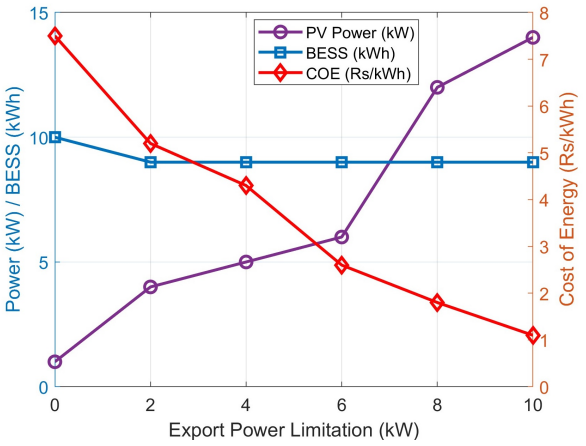

Figure 25. Sensitivity analysis for the impact of export power limitation.

Figure 26 represents the sensitivity analysis of the impact of TOU rates on a PV-BESS system, where the x-axis represents the TOU multiplier, and the y-axes represent power, BESS capacity, and the COE in Rs/kWh. As the TOU rates increase, the COE rises accordingly, reaching higher values at a TOU multiplier of 1.4. The PV capacity remains constant at around 10 kW across all TOU multipliers, showing minimal change. However, the optimal BESS capacity increases with higher TOU rates, indicating that more storage is needed to optimize cost savings when electricity prices fluctuate. The overall trend suggests that increasing TOU rates lead to higher costs of energy while incentivizing greater battery storage capacity to mitigate higher electricity prices.

7. Conclusion

This research paper presented a comparative analysis of the ideal sizing and cost minimization of grid-linked

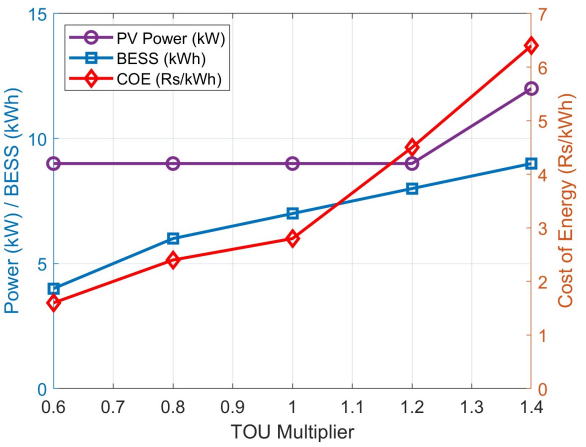

Figure 26. Sensitivity analysis for the impact of TOU rates.

https://dx.doi.org/10.57647/mjee.2026.2001.02

solar PV and BESS using two metaheuristic algorithms: PSO and APO, the comparison between them across different pricing schemes like Flat-Flat, TOU-Flat and Flat-TOU which demonstrates the superior performance of APO. For instance, under the Flat-Flat scheme, APO reduced the NPC_t from Rs 86,387.6783 (PSO) to Rs 38,266.7875, and the COE from Rs 18.58 per kWh to Rs 6.48 per kWh. Similarly, under the TOU-Flat scheme, APO achieved a lower NPC_t of Rs 36,389.309 compared to Rs 44,809.2447 for PSO, while reducing the COE from Rs 8.54 per kWh to Rs 7.93 per kWh. These results highlight APO's ability to optimize costs effectively while maintaining adequate energy generation and storage. Furthermore, APO consistently demonstrated better energy management, as seen in the Flat-TOU scenario, where it lowered the NPC_t from Rs 44,809.2447 (PSO) to Rs 36,389.309 and reduced the COE from Rs 11.46 per kWh to Rs 9.93 per kWh. APO also managed to balance energy exports and imports more efficiently, achieving 5.414 MWh of exported energy compared to 11.6839 MWh with PSO. The sensitivity analyses indicated that increasing the export power limitation, decreasing the import tariff and significantly reducing the COE.

Authors contributions
All authors contributed equally to the conception, design, execution, and writing of this work. All authors read and approved the final manuscript.

Availability of data and materials
The authors declare that the data supporting the findings of this study are available within the paper.

Conflict of interests
The authors assert that they do not have any identifiable conflicting financial interests or personal relationships that might be perceived to influence the work presented in this paper.

References

1. "**Ministry of New and Renewable Energy, Solar grid.**" Available from: https://mnre.gov.in/solar-grid-connected
2. "**Fraunhofer Institute for Solar Energy Systems ISE.**" Available from: https://www.ise.fraunhofer.de/en.html
3. Khenissi I, Fakhfakh MA, Sellami R, and Neji R. "**A new approach for optimal sizing of a grid connected PV system using PSO and GA algorithms: Case of Tunisia.**" Appl. Artif. Intell. 2021; 35:1930–51. DOI: 10.1080/08839514.2021.1995233
4. Garip S and Ozdemir S. "**Optimization of PV and battery energy storage size in grid-connected microgrid.**" Appl. Sci. 2022; 12:8247. DOI: 10.3390/app12168247
5. Regis N, Muriithi CM, and Ngoo L. "**Optimal battery sizing of a grid-connected residential photovoltaic system for cost minimization using PSO algorithm.**" Eng. Technol. Appl. Sci. Res. 2019; 9:4905–11. DOI: 10.48084/etasr.3094
6. Yi H and Yang X. "**A metaheuristic algorithm based on simulated annealing for optimal sizing and techno-economic analysis of PV systems with multi-type of battery energy storage.**" Sustain. Energy Technol. Assess. 2022; 53:102724. DOI: 10.1016/j.seta.2022.102724
7. Grisales-Norena LF, Ocampo-Toro JA, Montoya-Giraldo OD, Montano J, and Hernandez JC. "**Optimal operation of battery storage systems in standalone and grid-connected DC microgrids using parallel metaheuristic optimization algorithms.**" J. Energy Storage 2023; 65:107240. DOI: 10.1016/j.est.2023.107240
8. Fathima H and Palanisamy K. "**Optimized sizing, selection, and economic analysis of battery energy storage for grid-connected wind-PV hybrid system.**" Model. Simul. Eng. 2015; 2015:16. DOI: 10.1155/2015/713530
9. Nimma KS, Al-Falahi MD, Nguyen HD, Jayasinghe SDG, Mahmoud TS, and Negnevitsky M. "**Grey wolf optimization-based optimum energy-management and battery-sizing method for grid-connected microgrids.**" Energies 2018; 11:847. DOI: 10.3390/en11040847
10. Fares D, Fathi M, and Mekhilef S. "**Performance evaluation of metaheuristic techniques for optimal sizing of a stand-alone hybrid PV/wind/battery system.**" Appl. Energy 2022; 305:117823. DOI: 10.1016/j.apenergy.2021.117823
11. Zhao L, Jerbi H, Abbassi R, Liu B, Latifi M, and Nakamura H. "**Sizing renewable energy systems with energy storage systems based microgrids for cost minimization using hybrid shuffled frog-leaping and pattern search algorithm.**" Sustain. Cities Soc. 2021; 73:103124. DOI: 10.1016/j.scs.2021.103124
12. Nayak CK and Nayak MR. "**Optimal battery energy storage sizing for grid connected PV system using IHSA.**" Proc. Int. Conf. Signal Process., Commun., Power Embedded Syst. (SCOPES) 2016 :121–7. DOI: 10.1109/SCOPES.2016.7955654
13. Vaka SSKR and Matam SK. "**Optimal sizing and management of battery energy storage systems in microgrids for operating cost minimization.**" Electr. Power Compon. Syst. 2021; 49:1319–32. DOI: 10.1080/15325008.2022.2061641
14. Xu Y, Huang S, Wang Z, Ren Y, Xie Z, Guo J, and Zhu Z. "**Optimization based on tabu search algorithm for optimal sizing of hybrid PV/energy storage system: Effects of tabu search parameters.**" Sustain. Energy Technol. Assess. 2022; 53:102662. DOI: 10.1016/j.seta.2022.102662

15. Kamble R, Karve GM, Chakradeo A, and Vaidya G. "**Optimal sizing of battery energy storage system in microgrid by using particle swarm optimization technique.**" J. Integr. Sci. Technol. 2018; 6:6–12. Available from: https://pubs.iscience.in/journal/index.php/jist/article/viewFile/785/426

16. Hadi HA, Kassem A, Amoud H, Nadweh S, and Ghazaly NM. "**Using Grey Wolf Optimization Algorithm and Whale Optimization Algorithm for Optimal Sizing of Grid-Connected Bifacial PV Systems.**" J. Robot. Control 2024; 5:733–45. DOI: 18196/jrc.v5i3.21777

17. Jasim AM, Jasim BH, and Bures V. "**A novel grid-connected microgrid energy management system with optimal sizing using hybrid grey wolf and cuckoo search optimization algorithm.**" Front. Energy Res. 2022; 10:960141. DOI: 10.3389/fenrg.2022.960141

18. Diab AAZ, El-Rifaie AM, Zaky MM, and Tolba MA. "**Optimal sizing of stand-alone microgrids based on recent metaheuristic algorithms.**" Mathematics 2022; 10:140. DOI: 10.3390/math10010140

19. Salman UT, Al-Ismail FS, and Khalid M. "**Optimal sizing of battery energy storage for grid-connected and isolated wind-penetrated microgrid.**" IEEE Access 2020; 8:91129–38. DOI: 10.1109/ACCESS.2020.2992654

20. Mahmoud TS, Ahmed BS, and Hassan MY. "**The role of intelligent generation control algorithms in optimizing battery energy storage systems size in microgrids: A case study from Western Australia.**" Energy Convers. Manag. 2019; 196:1335–52. DOI: 10.1016/j.enconman.2019.06.045

21. Sun X, He H, and Ma L. "**Harmony search metaheuristic algorithm based on the optimal sizing of wind-battery hybrid micro-grid power system with different battery technologies.**" J. Energy Storage 2024; 75:109582. DOI: 10.1016/j.est.2023.109582

22. Diab AAZ, Sultan HM, Mohamed IS, Kuznetsov ON, and Do TD. "**Application of different optimization algorithms for optimal sizing of PV/wind/diesel/battery storage stand-alone hybrid microgrid.**" IEEE Access 2019; 7:119223–45. DOI: 10.1109/ACCESS.2019.2936656

23. Zhang Y, Ma T, and Yang H. "**A review on capacity sizing and operation strategy of grid-connected photovoltaic battery systems.**" Energy Built Environ. 2024; 5:500–16. DOI: 10.1016/j.enbenv.2023.04.001

24. Kumar J and Kumar N. "**Optimal scheduling of grid connected solar photovoltaic and battery storage system considering degradation cost of battery.**" Iran. J. Sci. Technol. Trans. Electr. Eng. 2022; 46:1175–88. DOI: 10.1007/s40998-022-00529-x

25. Boghdady TA, Bakhoum SR, and Sayed MM. "**Microgrid Optimal Sizing and Economic Operation for Rural Area in Assiut (Egypt) Using Meta-Heuristic Optimization Techniques.**" Proc. Int. Telecommun. Conf. (ITC-Egypt) 2022 :1–7. DOI: 10.1109/ITC-Egypt55520.2022.9855733

26. Khezri R, Mahmoudi A, and Aki H. "**Optimal planning of solar photovoltaic and battery storage systems for grid-connected residential sector: Review, challenges and new perspectives.**" Renew. Sustain. Energy Rev. 2022; 153:111763. DOI: 10.1016/j.rser.2021.111763

27. Li Y, Vilathgamuwa DM, Quevedo DE, Lee CF, and Zou C. "**Ensemble nonlinear model predictive control for residential solar battery energy management.**" IEEE Trans. Control Syst. Technol. 2023. DOI: 10.1109/TCST.2023.3291540

28. Li Y, Vilathgamuwa DM, Farrell TW, Tran NT, and Teague J. "**Nonlinear model predictive control of photovoltaic-battery system for short-term power dispatch.**" Proc. Annu. Conf. IEEE Ind. Electron. Soc. (IECON) 2018 :1884–9. DOI: 10.1109/IECON.2018.8591326

29. Mohamed MA, Shadoul M, Yousef H, Al-Abri R, and Sultan HM. "**Multi-agent based optimal sizing of hybrid renewable energy systems and their significance in sustainable energy development.**" Energy Rep. 2024; 12:4830–53. DOI: 10.1016/j.egyr.2024.10.051

30. Monteiro A et al. "**Development of a tool for sizing and technical–financial analysis of energy-storage systems using batteries.**" Energy Technol. 2024; 12:2301638. DOI: 10.1002/ente.202301638

31. Jaiswal D, Mittal M, and Mittal V. "**An optimization approach to enhance performance of a solar PV system based on performance assessment of an existing 5 MW on-grid PV system.**" J. Harbin Eng. Univ. 2023; 44. Available from: https://harbinengineeringjournal.com/index.php/journal/article/download/628/473/1091

32. Wang X, Snasel V, Mirjalili S, Pan JS, Kong L, and Shehadeh HA. "**Artificial Protozoa Optimizer (APO): A novel bio-inspired metaheuristic algorithm for engineering optimization.**" Knowl. Based Syst. 2024 :111737. DOI: 10.1016/j.knosys.2024.111737